

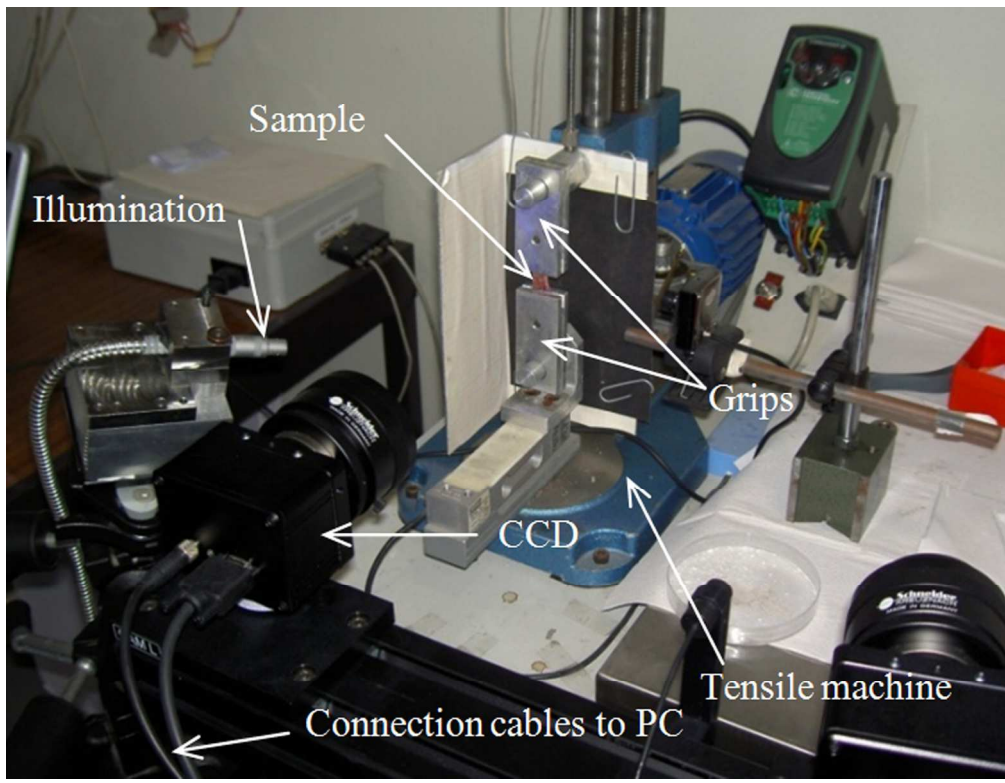


**A HYBRID METHOD TO CHARACTERIZE THE MECHANICAL BEHAVIOUR OF BIOLOGICAL HYPER-ELASTIC TISSUES**

Journal:	<i>Computer Methods in Biomechanics and Biomedical Engineering: Imaging &amp; Visualization</i>
Manuscript ID:	TCIV-2014-0095.R3
Manuscript Type:	Research Manuscripts
Date Submitted by the Author:	21-Mar-2015
Complete List of Authors:	Ribeiro, João; Polytechnic Institute of Bragança, Mechanical Technology Lopes, Hernâni; ISEP, Polytechnic Institute of Porto, Martins, Pedro; Faculdade de Engenharia da Universidade do Porto,
Keywords:	Imaging and Visualization in Biomechanics, Image Processing and Analysis, Software Development for Imaging and Visualization

SCHOLARONE™  
Manuscripts

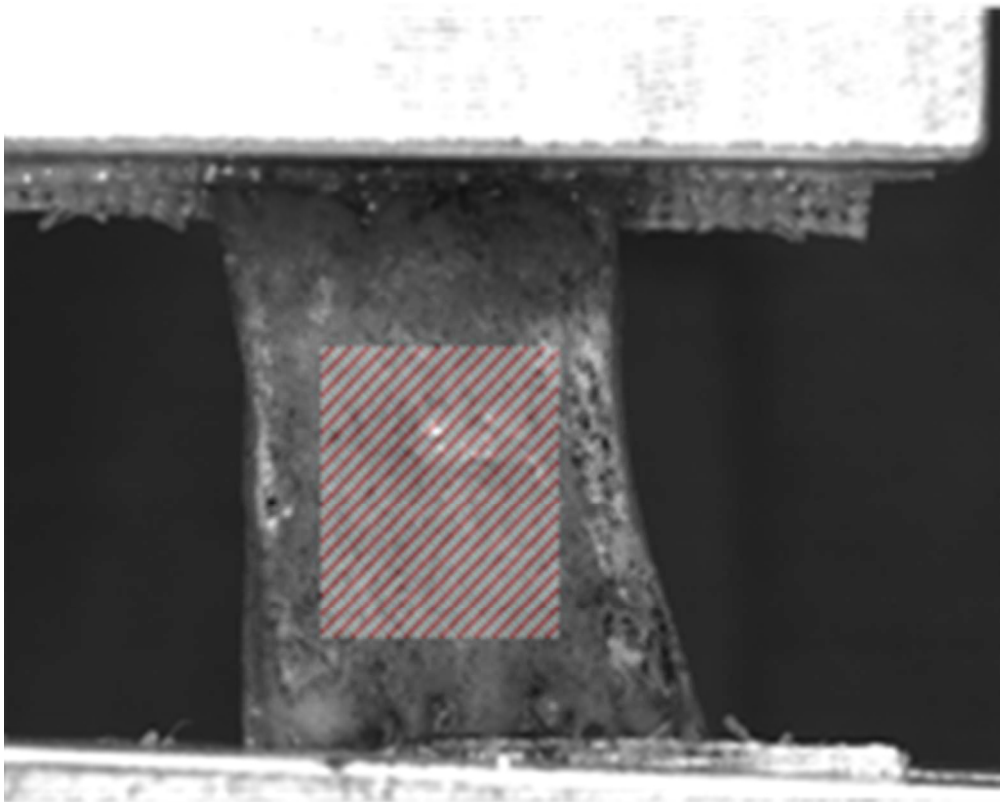
1  
2  
3  
4  
5  
6  
7  
8  
9  
10  
11  
12  
13  
14  
15  
16  
17  
18  
19  
20  
21  
22  
23  
24  
25  
26  
27  
28  
29  
30  
31  
32  
33  
34  
35  
36  
37  
38  
39  
40  
41  
42  
43  
44  
45  
46  
47  
48  
49  
50  
51  
52  
53  
54  
55  
56  
57  
58  
59  
60



253x195mm (300 x 300 DPI)

Preview Only

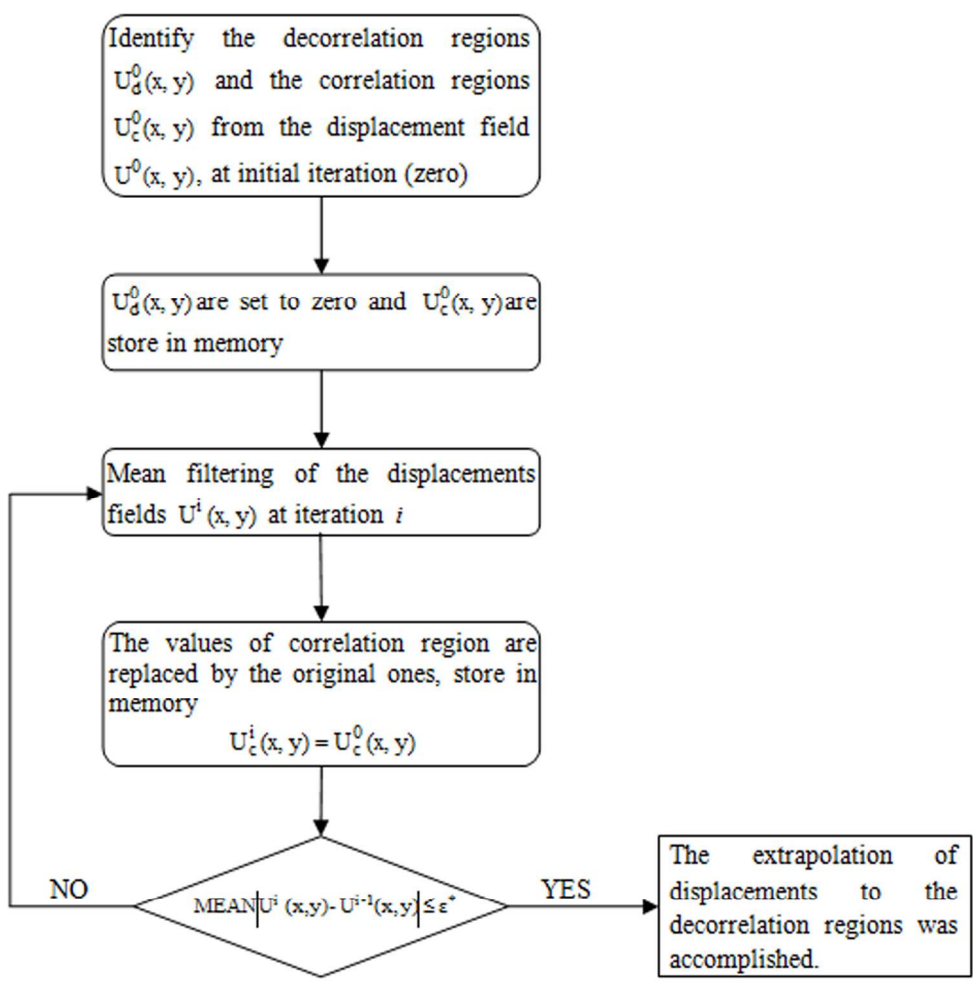
1  
2  
3  
4  
5  
6  
7  
8  
9  
10  
11  
12  
13  
14  
15  
16  
17  
18  
19  
20  
21  
22  
23  
24  
25  
26  
27  
28  
29  
30  
31  
32  
33  
34  
35  
36  
37  
38  
39  
40  
41  
42  
43  
44  
45  
46  
47  
48  
49  
50  
51  
52  
53  
54  
55  
56  
57  
58  
59  
60



161x135mm (300 x 300 DPI)

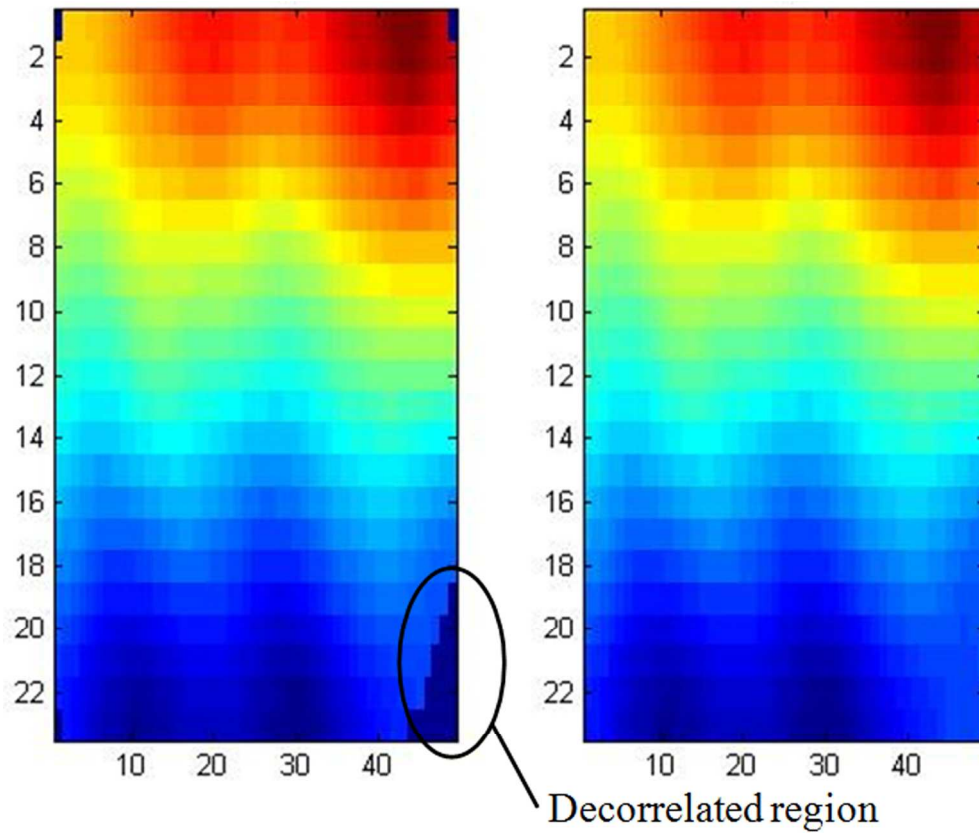
View Only

1  
2  
3  
4  
5  
6  
7  
8  
9  
10  
11  
12  
13  
14  
15  
16  
17  
18  
19  
20  
21  
22  
23  
24  
25  
26  
27  
28  
29  
30  
31  
32  
33  
34  
35  
36  
37  
38  
39  
40  
41  
42  
43  
44  
45  
46  
47  
48  
49  
50  
51  
52  
53  
54  
55  
56  
57  
58  
59  
60



186x186mm (300 x 300 DPI)

only

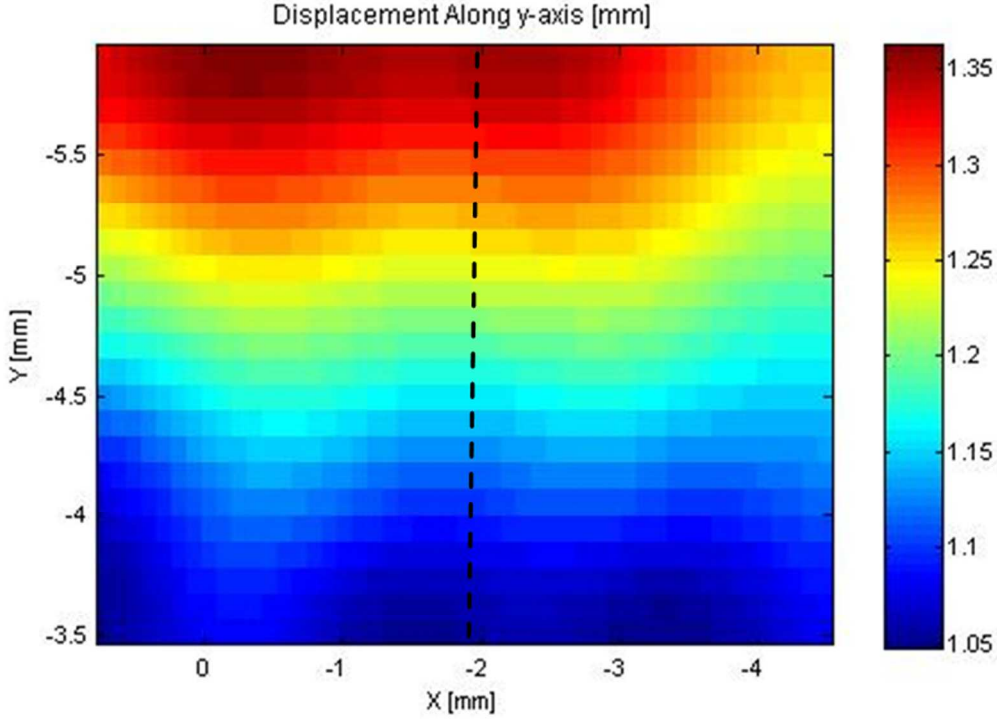


230x193mm (300 x 300 DPI)

View Only

1  
2  
3  
4  
5  
6  
7  
8  
9  
10  
11  
12  
13  
14  
15  
16  
17  
18  
19  
20  
21  
22  
23  
24  
25  
26  
27  
28  
29  
30  
31  
32  
33  
34  
35  
36  
37  
38  
39  
40  
41  
42  
43  
44  
45  
46  
47  
48  
49  
50  
51  
52  
53  
54  
55  
56  
57  
58  
59  
60

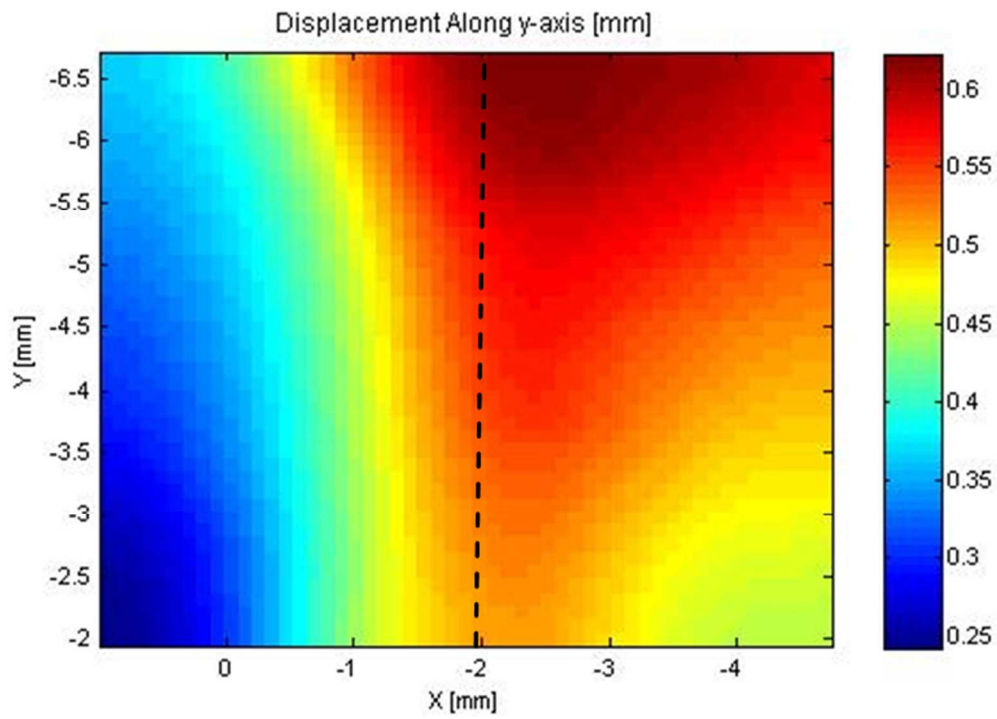
1  
2  
3  
4  
5  
6  
7  
8  
9  
10  
11  
12  
13  
14  
15  
16  
17  
18  
19  
20  
21  
22  
23  
24  
25  
26  
27  
28  
29  
30  
31  
32  
33  
34  
35  
36  
37  
38  
39  
40  
41  
42  
43  
44  
45  
46  
47  
48  
49  
50  
51  
52  
53  
54  
55  
56  
57  
58  
59  
60



271x195mm (300 x 300 DPI)

view Only

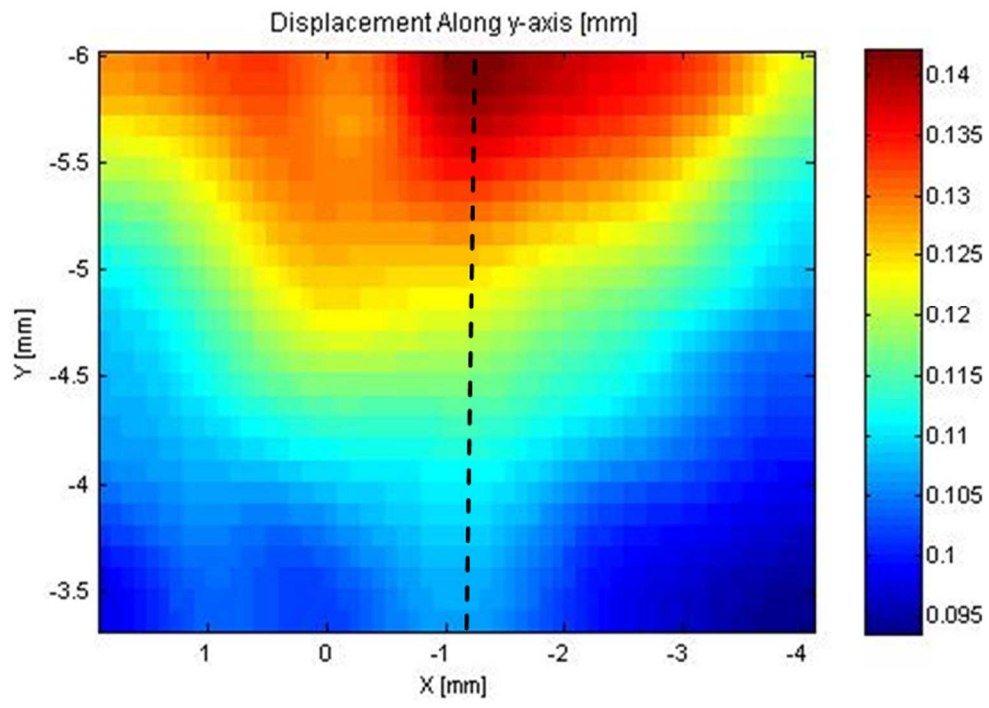
1  
2  
3  
4  
5  
6  
7  
8  
9  
10  
11  
12  
13  
14  
15  
16  
17  
18  
19  
20  
21  
22  
23  
24  
25  
26  
27  
28  
29  
30  
31  
32  
33  
34  
35  
36  
37  
38  
39  
40  
41  
42  
43  
44  
45  
46  
47  
48  
49  
50  
51  
52  
53  
54  
55  
56  
57  
58  
59  
60



272x193mm (300 x 300 DPI)

view Only

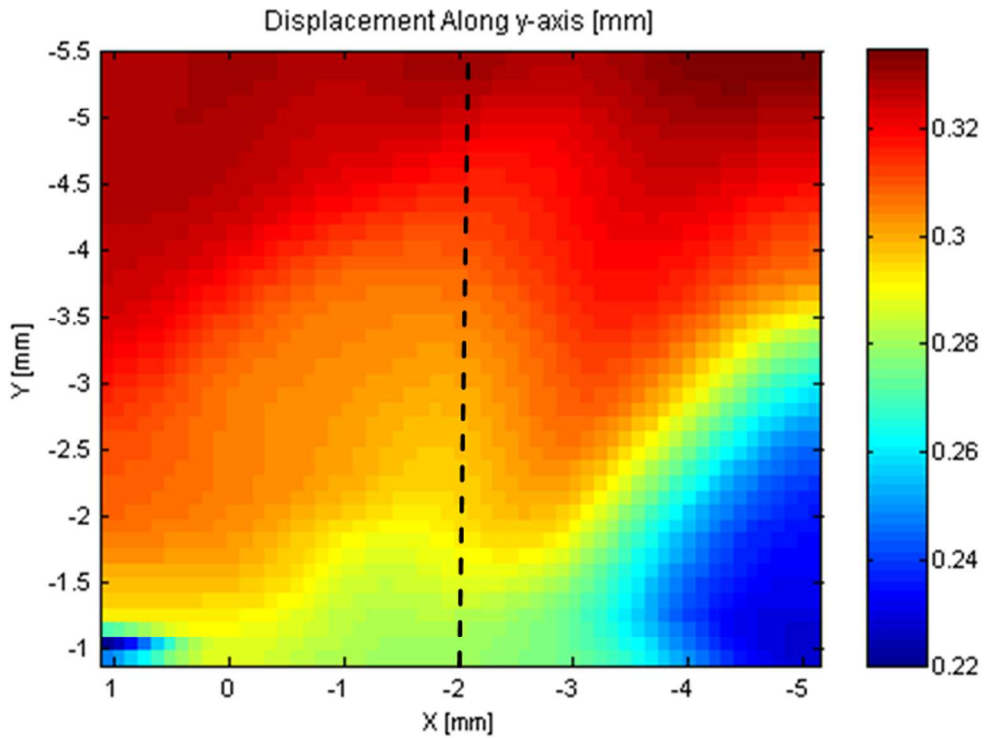
1  
2  
3  
4  
5  
6  
7  
8  
9  
10  
11  
12  
13  
14  
15  
16  
17  
18  
19  
20  
21  
22  
23  
24  
25  
26  
27  
28  
29  
30  
31  
32  
33  
34  
35  
36  
37  
38  
39  
40  
41  
42  
43  
44  
45  
46  
47  
48  
49  
50  
51  
52  
53  
54  
55  
56  
57  
58  
59  
60



278x193mm (300 x 300 DPI)

view Only

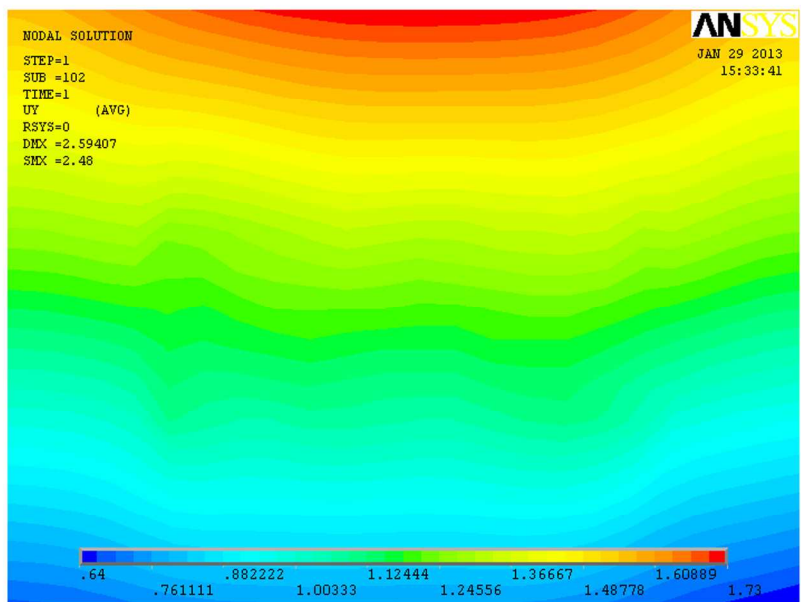




262x194mm (300 x 300 DPI)

1  
2  
3  
4  
5  
6  
7  
8  
9  
10  
11  
12  
13  
14  
15  
16  
17  
18  
19  
20  
21  
22  
23  
24  
25  
26  
27  
28  
29  
30  
31  
32  
33  
34  
35  
36  
37  
38  
39  
40  
41  
42  
43  
44  
45  
46  
47  
48  
49  
50  
51  
52  
53  
54  
55  
56  
57  
58  
59  
60

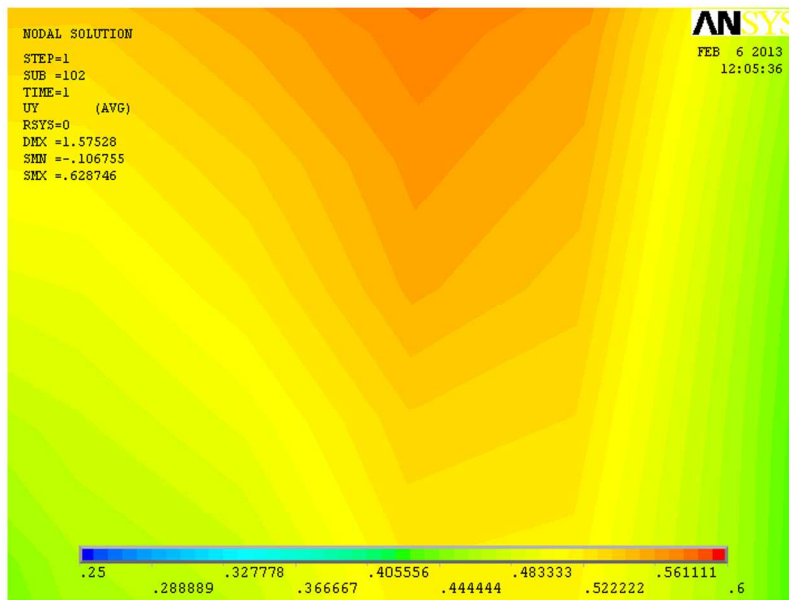
1  
2  
3  
4  
5  
6  
7  
8  
9  
10  
11  
12  
13  
14  
15  
16  
17  
18  
19  
20  
21  
22  
23  
24  
25  
26  
27  
28  
29  
30  
31  
32  
33  
34  
35  
36  
37  
38  
39  
40  
41  
42  
43  
44  
45  
46  
47  
48  
49  
50  
51  
52  
53  
54  
55  
56  
57  
58  
59  
60



316x197mm (300 x 300 DPI)

Review Only

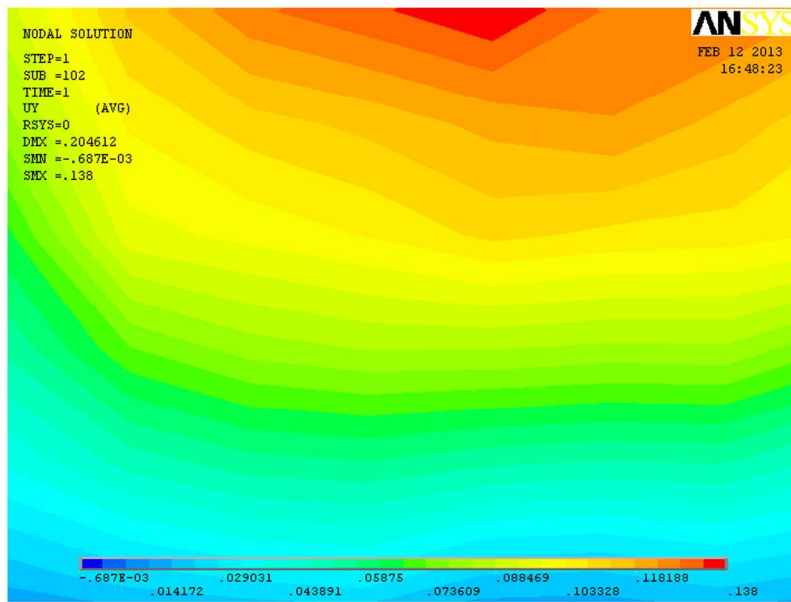
1  
2  
3  
4  
5  
6  
7  
8  
9  
10  
11  
12  
13  
14  
15  
16  
17  
18  
19  
20  
21  
22  
23  
24  
25  
26  
27  
28  
29  
30  
31  
32  
33  
34  
35  
36  
37  
38  
39  
40  
41  
42  
43  
44  
45  
46  
47  
48  
49  
50  
51  
52  
53  
54  
55  
56  
57  
58  
59  
60



316x197mm (300 x 300 DPI)

Review Only

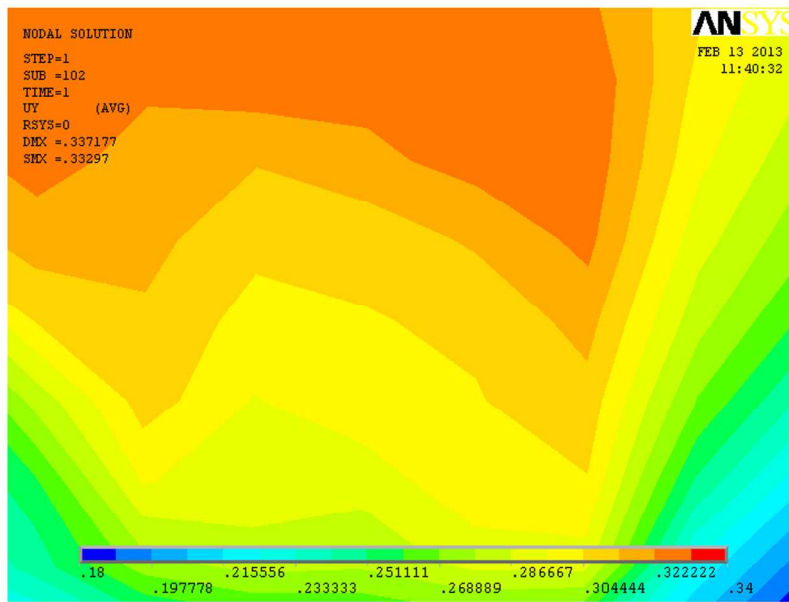
1  
2  
3  
4  
5  
6  
7  
8  
9  
10  
11  
12  
13  
14  
15  
16  
17  
18  
19  
20  
21  
22  
23  
24  
25  
26  
27  
28  
29  
30  
31  
32  
33  
34  
35  
36  
37  
38  
39  
40  
41  
42  
43  
44  
45  
46  
47  
48  
49  
50  
51  
52  
53  
54  
55  
56  
57  
58  
59  
60



316x197mm (300 x 300 DPI)

Review Only

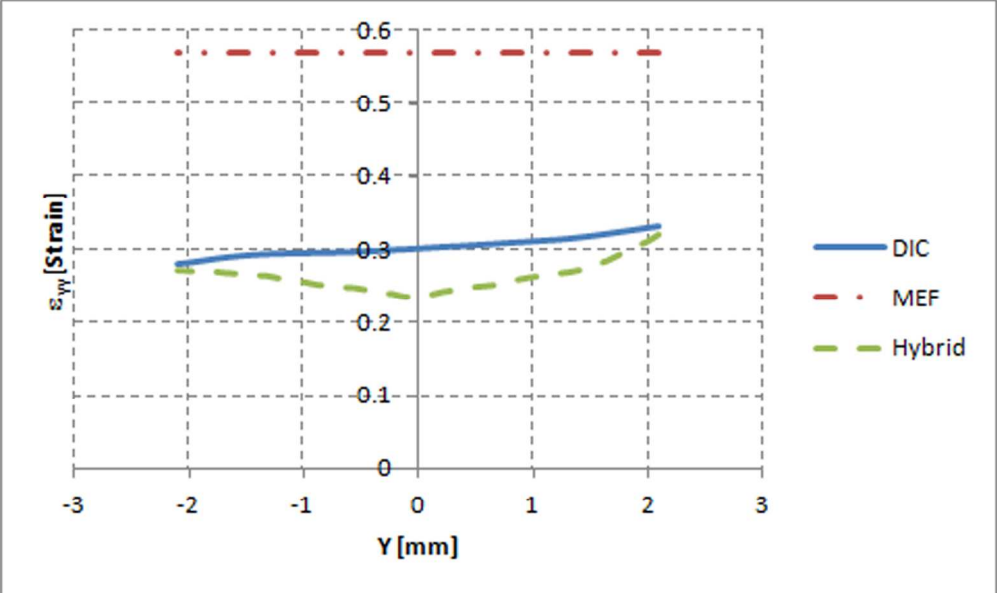
1  
2  
3  
4  
5  
6  
7  
8  
9  
10  
11  
12  
13  
14  
15  
16  
17  
18  
19  
20  
21  
22  
23  
24  
25  
26  
27  
28  
29  
30  
31  
32  
33  
34  
35  
36  
37  
38  
39  
40  
41  
42  
43  
44  
45  
46  
47  
48  
49  
50  
51  
52  
53  
54  
55  
56  
57  
58  
59  
60



316x197mm (300 x 300 DPI)

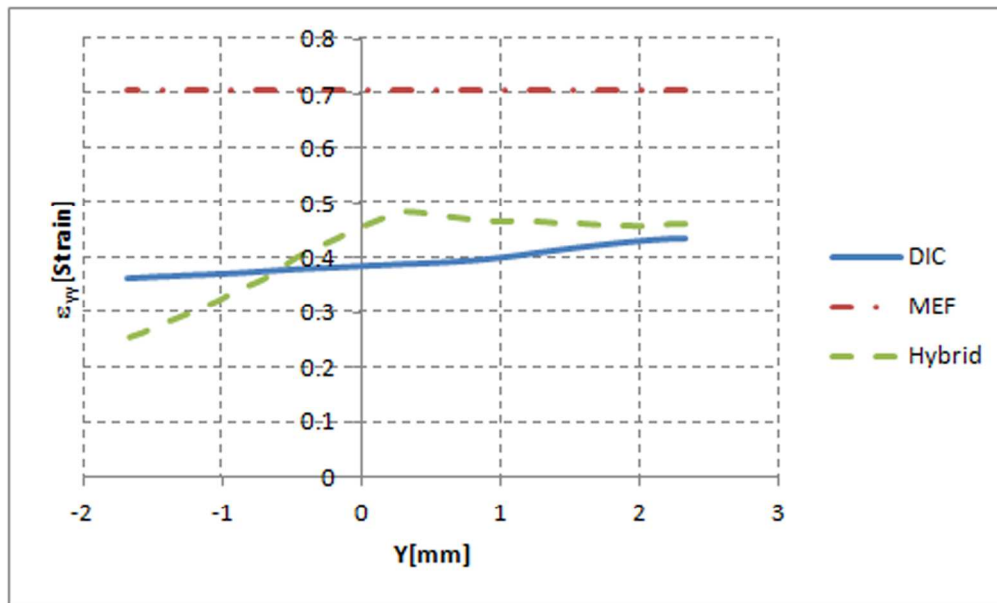
Review Only

1  
2  
3  
4  
5  
6  
7  
8  
9  
10  
11  
12  
13  
14  
15  
16  
17  
18  
19  
20  
21  
22  
23  
24  
25  
26  
27  
28  
29  
30  
31  
32  
33  
34  
35  
36  
37  
38  
39  
40  
41  
42  
43  
44  
45  
46  
47  
48  
49  
50  
51  
52  
53  
54  
55  
56  
57  
58  
59  
60



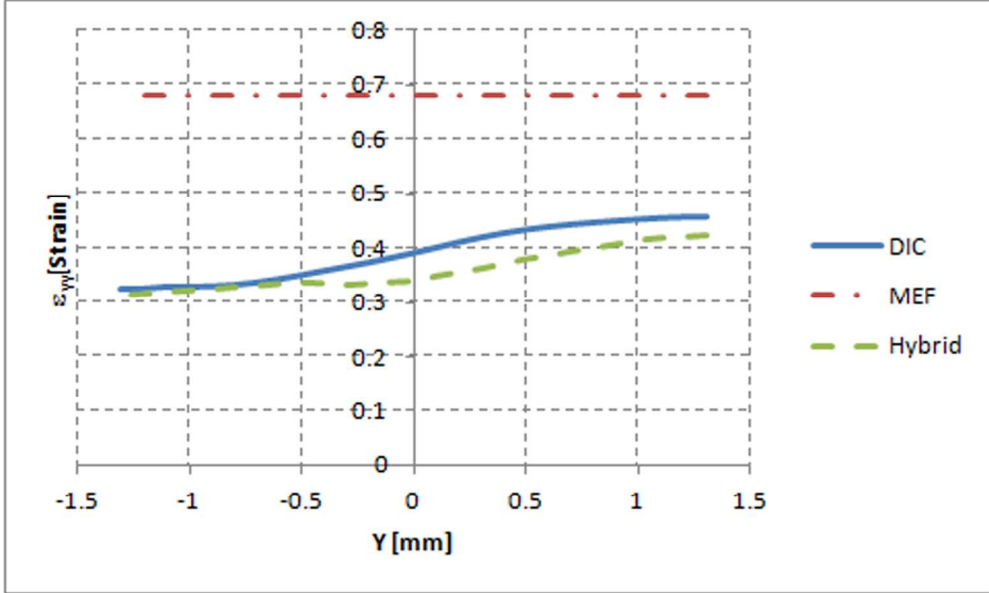
170x102mm (300 x 300 DPI)

Review Only



170x102mm (300 x 300 DPI)

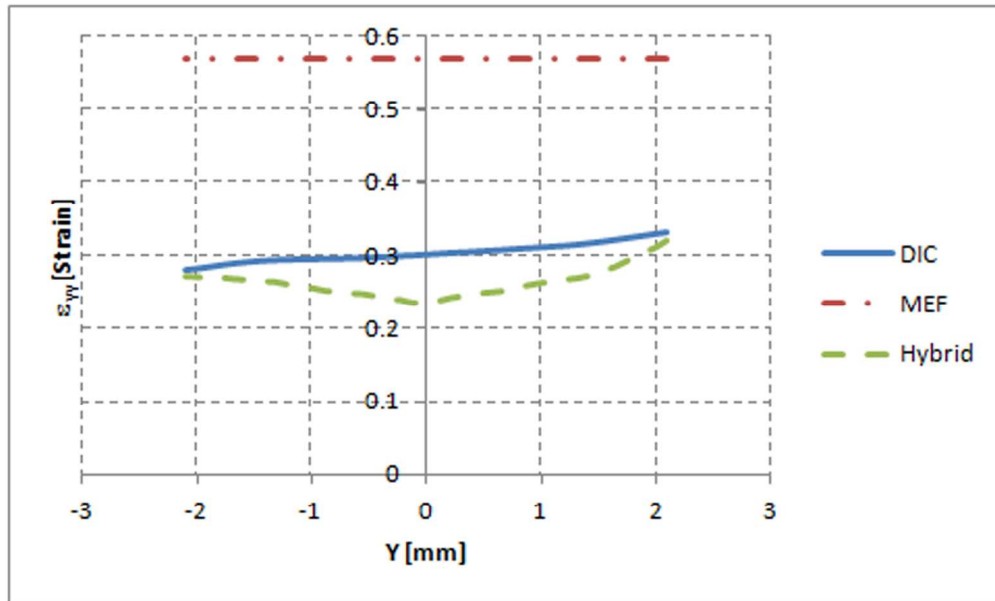
1  
2  
3  
4  
5  
6  
7  
8  
9  
10  
11  
12  
13  
14  
15  
16  
17  
18  
19  
20  
21  
22  
23  
24  
25  
26  
27  
28  
29  
30  
31  
32  
33  
34  
35  
36  
37  
38  
39  
40  
41  
42  
43  
44  
45  
46  
47  
48  
49  
50  
51  
52  
53  
54  
55  
56  
57  
58  
59  
60



171x102mm (300 x 300 DPI)

Review Only





170x102mm (300 x 300 DPI)

1  
2  
3  
4  
5  
6  
7  
8  
9  
10  
11  
12  
13  
14  
15  
16  
17  
18  
19  
20  
21  
22  
23  
24  
25  
26  
27  
28  
29  
30  
31  
32  
33  
34  
35  
36  
37  
38  
39  
40  
41  
42  
43  
44  
45  
46  
47  
48  
49  
50  
51  
52  
53  
54  
55  
56  
57  
58  
59  
60

<i>Samples</i>	<i>Thickness [mm]</i>	<i>Length [mm]</i>	<i>Width [mm]</i>
1	1.348	13.077	9.619
2	1.686	11.159	7.414
3	1.687	8.514	9.273
4	2.810	13.108	9.150

339x151mm (300 x 300 DPI)

er Review Only

---

*Samples Displacement [mm]*

---

1	2.48
---	------

---

2	0.81
---	------

---

3	0.60
---	------

---

4	0.77
---	------

---

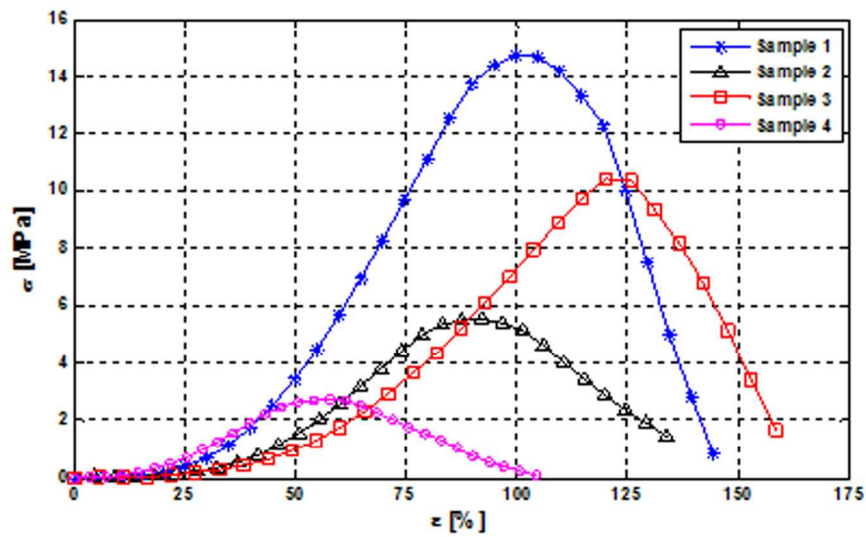
191x152mm (300 x 300 DPI)

ew Only

<i>Sample</i>	<i>Hybrid Method</i> [%]	<i>FEM</i> [%]
1	6.92	49.7
2	15.6	81
3	7.47	77.2
4	13.2	88.9

245x151mm (300 x 300 DPI)

Review Only



163x92mm (300 x 300 DPI)

1  
2  
3 **A HYBRID METHOD TO CHARACTERIZE THE MECHANICAL**  
4 **BEHAVIOUR OF BIOLOGICAL HYPER-ELASTIC TISSUES**  
5  
6

7 João Ribeiro<sup>a</sup>, Hernâni Lopes<sup>b</sup>, Pedro Martins<sup>c</sup>  
8  
9

10 <sup>a</sup> *Polytechnic Institute of Bragança, Bragança, Portugal, jribeiro@ipb.pt*  
11

12 <sup>b</sup> *ISEP, Polytechnic Institute of Porto, Porto, Portugal*  
13  
14

15 <sup>c</sup> *IDMEC, FEUP, Porto, Portugal*  
16  
17  
18  
19  
20  
21  
22  
23  
24  
25  
26  
27  
28  
29  
30  
31  
32  
33  
34  
35  
36  
37  
38  
39  
40  
41  
42  
43  
44  
45  
46  
47  
48  
49  
50  
51  
52  
53  
54  
55  
56  
57  
58  
59  
60

## A HYBRID METHOD TO CHARACTERIZE THE MECHANICAL BEHAVIOUR OF BIOLOGICAL HYPER-ELASTIC TISSUES

**Abstract.** The characterization of biological tissues has become high interest area in recent years, due to the grow uses and development of artificial soft tissues implants. These tissues present a non-linear mechanical behavior, which highly differs from typical engineering materials. This aspect brings us an enormous difficulty in characterization of soft tissues and thus required the development of new experimental techniques associated to new numerical algorithms. This work presents the mechanical characterization of human vaginal mucosa based on a hybrid technique that combines the experimental measurement of displacement field, acquired during a tensile test with numerical simulation, using material constitutive laws. The Digital Image Correlation technique was used for high spatial resolution measurement of the displacements field on the hyper-elastic biological tissues. Several numerical simulations were carryout based on finite element commercial package, Ansys®, by combining the experimental displacements with different hyper-elastic models, which were developed from the experimental tensile test. Fluid release from specimen was observed during the tensile test, producing speckle decorrelation and, therefore, lack of information in displacement field. This problem was overcome by extrapolating data at the boundaries, through the application of special algorithm developed by the authors. The proposed hybrid method show to be more acquired then the numerical method based only on material constitutive models.

Keywords: Hyper-elastic tissues, Digital Image Correlation, Finite elements method, Image processing

### 1. Introduction

Many biological tissues present a high nonlinear elastic behaviour, which is characterized by hyper-elastic or viscoelastic constitutive relations. They present heterogeneous mechanical properties that can be associated to the orientation, length and thickness of the tissue fibres. In order to identify the mechanical global properties of biological tissues, several methodologies have been proposed in literature [1-7]. One

1  
2  
3 of the most used techniques is based on building a different constitutive model for each  
4  
5  
6  
7  
8  
9  
10  
11  
12  
13  
14  
15  
16  
17  
18  
19  
20  
21  
22  
23  
24  
25  
26  
27  
28  
29  
30  
31  
32  
33  
34  
35  
36  
37  
38  
39  
40  
41  
42  
43  
44  
45  
46  
47  
48  
49  
50  
51  
52  
53  
54  
55  
56  
57  
58  
59  
60  
of the most used techniques is based on building a different constitutive model for each  
fiber orientation and each region of the biological tissue. This procedure requires a  
large number of tensile tests and the measurement of stress-strain curve. Besides the  
need of expensive equipments, this is highly time consuming task due to the large  
number of samples preparation and the performance of their experimental tests.

However, this afford is compensated by allowing the numerical simulations of material  
behaviour with an accuracy that depends on the detail of experimental measurement.  
Therefore, only a high spatial resolution of the specimen will allow building a reliable  
numerical model to simulate the mechanical behaviour of such materials [7-11].

The mechanical behavior of soft biological tissues can be approached by the  
constitutive models that characterize the hyper-elastic materials. In order to study these  
materials, it was developed the non-linear elasticity theory [12]. In this theory, a hyper-  
elastic material, also known as the Green elastic material is defined as the one for which  
there is a Helmholtz free energy function [13], also called the strain energy or stored  
energy that describes the behavior in terms of mechanical energy for this class of  
materials.

Traditionally, the experimental determination of some mechanical properties of  
the hyper-elastic biological tissues has been performed using conventional techniques,  
which were previously developed for the study of homogenous and isotropic materials  
[6]. However, these experimental techniques show to be inadequate for the mechanical  
characterization of heterogeneous materials, like biological ones, and only the average  
properties can be identified through this test. Therefore, full-field measurements are  
needed for detailed analysis of mechanical behavior, being the optical techniques the  
most suited for this purpose. These allow the non-contact, full-field and high resolution  
measurement of displacement and strain fields. The optical techniques were essentially



1  
2  
3 developed in last two decades and are based on digital image recording system. One of  
4  
5 **the most widely used technique** is the Digital Image Correlation (DIC), which was  
6  
7 initially developed by Sutton et al. [14, 15, 16, 17] and Bruck et al. [18]. The factor that  
8  
9 most contributed to popularity of this technique was its high resolution, the use of white  
10  
11 light and simple surface preparation. The measurements are performed based on the  
12  
13 correlation between random intensity patterns. The displacements and **strain fields are**  
14  
15 **evaluated** in small areas with distinctive speckle pattern. For this purpose, the image is  
16  
17 initially subdivided into smaller regions. The displacements and the strain fields are  
18  
19 evaluated during loading of the specimen in each region by correlation of the speckle  
20  
21 pattern between different digital recorded images [19]. The speckle pattern can be the  
22  
23 natural texture of the surface or artificially created by special painting. The speckle  
24  
25 pattern size, the dispersion and image contrast can influence the accuracy of the  
26  
27 measurement [20]. The best results are achieved when using smaller speckle size,  
28  
29 random distribution and high image contrast. In this particular technique, the spatial  
30  
31 resolution of the speckle pattern and the ability of the algorithm to solve the image at  
32  
33 sub-pixel level have **an important role in the accuracy of the measurements**. In order to  
34  
35 reach higher accuracy, correlations are based on squares of pixels, known as facets,  
36  
37 rather than individual pixel tracing. These facets are represented by an array of  
38  
39 grayscale values, which correspond to the speckle pattern. In general, a single camera is  
40  
41 sufficient to perform two dimensional measurements in the object surface [21], and two  
42  
43 or more cameras are needed for three dimensional measurements [22]. In the market,  
44  
45 there are available commercial integrated systems with different measurement  
46  
47 resolution and accuracy. Some examples of these systems are: Q-400 DIC of Dantec  
48  
49 Dynamics, VIC-3D of Correlated Solutions and Aramis of Gom, used in this work.  
50  
51  
52  
53  
54  
55  
56  
57  
58  
59  
60

1  
2  
3 The digital image correlation has the sensibility range that could allow the  
4 measurement of such large displacements. However, the strain fields are computed by  
5 the differentiation of displacement fields and this technique could amplify the image  
6 noise, in this case the quality of strain fields are not adequate. Due to these limitations,  
7 in this work it was developed, a hybrid method which uses the displacement field  
8 obtained with DIC applied in the nodes of a finite element model in order to overcome  
9 the limitations associated with large displacements.  
10  
11  
12  
13  
14  
15  
16  
17  
18  
19

## 20 **2. Methods**

### 21 **2.1. Experimental Tests**

22  
23  
24  
25 In the experimental work it was used human vaginal mucosa tissue of same  
26 patient with 65 years old. In this experimental test the material was subjected to a  
27 tensile test and simultaneously a sequence of images of the sample face were captured  
28 by a CCD camera. These images are used to obtain the displacement and strain fields  
29 using commercial DIC software (Aramis of Gom). Prior to the experimental test the  
30 tissue suffered a previous preparation in two stages; firstly it was cut in rectangular  
31 shape with the dimensions indicated in table 1 and then applied a random speckle with  
32 toner powder on one of the sample faces. The experimental work was made in  
33 laboratory environment where the temperature and the relative humidity were 20°C and  
34 50%, respectively.  
35  
36  
37  
38  
39  
40  
41  
42  
43  
44  
45  
46  
47  
48

49 Table 1 – Dimensions of the tested samples.

50  
51  
52  
53 The tissue was mounted in the tensile machine using grips specially designed to  
54 prevent slippage of the sample with the face with the random speckle pattern facing the  
55 CCD camera. The measurement quality obtained by DIC depends essentially of camera  
56  
57  
58  
59  
60

1  
2  
3 resolution, quality of speckle, image contrast and definition. To improve the last  
4  
5 characteristic, without changing the moisture of the samples, a cold light was employed,  
6  
7 see Fig. 1. The in-plane displacement field measurement needs one camera and the  
8  
9 acquisition rates for these tests were one image per second, for a total of 150 seconds.  
10  
11 The images acquired during the tensile tests were sent to the computer and processed  
12  
13 using the DIC software. The computation of the displacement and strain field needs a  
14  
15 previous calibration of the measurements, for this purpose, a strip of graph paper was  
16  
17 used, fixed on one of the grips.  
18  
19

20  
21  
22 (a)

23  
24  
25 (b)

26  
27 Fig.1 Optical and tensile test set-up, using DIC to obtain the displacement field  
28  
29 measurement (a) and detail of the sample with the analysis region (b).

30  
31 Despite all images are acquired during the loading test, only the correspondent  
32  
33 to the low load levels could be used in this analysis due to fluid release by the samples.  
34  
35 This phenomenon caused disturbance in speckle pattern, resulting in the decorrelation  
36  
37 of important regions on the samples. Thus, in order to overcome this problem and use  
38  
39 the entire regions in the analysis, the acquired data were post-processed using dedicate  
40  
41 algorithm developed by the authors. The displacement and strain fields are filtered in  
42  
43 order to reduce the experimental noise and eliminate uncorrelated areas. This is  
44  
45 performed by applying a smart median filter algorithm, which preserves the correlated  
46  
47 information and extrapolates the boundary information to the uncorrelated areas. The  
48  
49 algorithm is described in the following schematic diagram (see Fig. 3).  
50  
51

52  
53 Despite the solution to fill the lost regions, the algorithm has some physical  
54  
55 limitations because it depends of the decorrelated regions dimensions. So, if the  
56  
57  
58  
59  
60

1  
2  
3 decorrelated region is too large (higher than thirty percent of the image) it is not  
4  
5 possible to obtain the complete measurements of displacement and strain fields.  
6  
7

## 8 9 2.2. *Finite element model*

10  
11 The numerical simulations were implemented by commercial FEM (finite  
12  
13 element method) software (Ansys®). For the numerical simulations, specific  
14  
15 constitutive models developed to simulate the hyper-elastic materials behavior, were  
16  
17 applied. The constitutive models tested in this work were the Mooney-Rivlin [23],  
18  
19 Ogden [24] and Yeoh [25] models, because usually they characterize with accuracy the  
20  
21 mechanical behavior of the hyper-elastic materials. However, the tests had shown that  
22  
23 the Yeoh model fits reasonably to the study of vaginal tissues. Already a polynomial  
24  
25 model as Ogden has, in principle, more plasticity since it is possible increases the model  
26  
27 by adding more terms in the series whenever the complexity of experimental data  
28  
29 requires. For the Mooney-Rivlin model it is possible to use the same principle although  
30  
31 the incompressible form has only two constants. For these reasons, the Ogden model  
32  
33 was used in this work. The strain energy density ( $\Psi$ ) for this model is described by the  
34  
35 follow expression [26]:  
36  
37  
38  
39  
40

$$41 \Psi = \sum_{i=1}^N \frac{\mu_i}{\alpha_i} (\lambda_1^{\alpha_i} + \lambda_2^{\alpha_i} + \lambda_3^{\alpha_i} - 3) \quad (1)$$

42  
43  
44  
45

46  
47 where  $N$  is a positive integer which determines the number of terms in the strain-energy  
48  
49 function,  $\mu_i$  are (constant) shear moduli and  $\alpha_i$  are dimensionless constants,  $i = 1, \dots, N$   
50  
51 and  $\lambda_1, \lambda_2, \lambda_3$  are the principal stretches.

52 The material constants were calibrated based on the experimental results,  
53  
54 obtained by the experimental curves of tensile test. These curves are represented in Fig.  
55  
56  
57  
58  
59  
60

1  
2  
3 2. Each curve was used to determine the respective material constant calibration of  
4  
5 sample.  
6  
7

8  
9 Fig.2 The obtained stress-strain curves in the tensile test for the four tested samples.

10  
11 The geometry of the sample used experimentally was modeled to implement the  
12  
13 numerical and the mesh was generated. The Ogden model that describes a nonlinear  
14  
15 hyperelastic behavior was chosen in the simulation. Verifying the equation (1) it is  
16  
17 possible to observe the need of determining the material constants, for that purpose was  
18  
19 employed in the simulation the experimental curve of tensile test. It generated a mesh of  
20  
21 quadratic elements and isoparametric with 8-node [27], this type of element is referred  
22  
23 as PLANE183 [28].  
24  
25

26  
27 For the boundary conditions, the bottom edge was clamped and constant  
28  
29 displacements in vertical direction on the upper edge of the model.  
30

31 Analyzing the stress-strain curves of the four tested samples, Fig. 2, it can be  
32  
33 seen that the samples have different behaviors during the test. Due to this fact,  
34  
35 simulations were made for different values of applied displacements. In table 2 are  
36  
37 shown the displacements used for the numerical simulations. . These values  
38  
39 corresponded to the maximum displacement that DIC system could measure before the  
40  
41 speckle loss due to the fluid release of the samples.  
42  
43  
44

45  
46 Table 2 – Applied displacements in the numerical simulations.  
47  
48

49 The displacements values were the same that were used in experimental tests.  
50  
51

### 52 53 2.3. Hybrid method

54  
55 The hybrid method proposed in this work was developed to improve the  
56  
57 reliability of numerical model in reproduction of the mechanical behaviour of biological  
58  
59  
60

1  
2  
3 soft tissues during tensile test. This method used the constitutive hyper-elastic material  
4 model and the displacement fields in two orthogonal directions (x,y), measured with the  
5 DIC technique for the time instant of tensile test (Table 2), and applies them on the  
6 nodes in the numerical model. This is accomplished by adjusting the experimental  
7 displacements fields to the location of the nodes in the numerical model through the  
8 interpolation experimental displacements using cubic spline interpolation functions.  
9

10  
11  
12  
13  
14  
15  
16 However, the speckle decorrelation led to the partial loss of the experimental  
17 displacement field, measured during the tensile test. To overcome this problem a new  
18 approach is proposed in this work. This is based on the extrapolation of experimental  
19 displacement to the decorrelation regions without changing experimental values. The  
20 Fig. 3 shows the schematic diagram of the iterative procedure used for the extrapolation.  
21  
22 Firstly, the original experimental displacements, from the correlation regions, are store  
23 in memory and the decorrelation regions are replaced by zero values. For each iteration,  
24 a low-pass is first applied to this displacement fields, using mean filtering with 3×3  
25 square kernel, and then the correlation regions are replaced by the original experimental  
26 displacements. This procedure is repeated until a predefined threshold error  $\epsilon^*$  is  
27 reached, computed from the mean differences between two consecutive displacement  
28 fields. One should note that the results with this procedure are highly dependent on the size of  
29 the decorrelation regions relatively to the displacement field. So, it is expected to obtain a  
30 better result for small decorrelation areas.  
31  
32  
33  
34  
35  
36  
37  
38  
39  
40  
41  
42  
43  
44  
45  
46  
47  
48  
49

50 Fig 3. The algorithm for extrapolation of displacements to the decorrelation regions.

51  
52 The Fig. 4 shows the application of the proposed procedure to the extrapolation of  
53 experimental displacements to the decorrelation region, corresponding a 2% of the  
54 measurement area. After the application of the proposed procedure is obtain a continues  
55  
56  
57  
58  
59  
60

1  
2  
3 and smooth extrapolation of the displacements field. The procedure convergence is  
4 relatively fast and a small mean error of 0.1% is reached after 10 iterations.  
5  
6  
7  
8

9 (a)

(b)

10  
11 Fig 4. Displacement field obtained with DIC before (a) and after (b) data treatment.

12 **At the end of this process an array of displacements is generated** which could be  
13 directly used in ANSYS® software.  
14  
15  
16  
17  
18

### 19 3. Results

20  
21 **The figures below show the displacement and strain results obtained with the**  
22 **proposed hybrid method, where digital image correlation data and the numerical**  
23 **simulation results using FEM are applied.**  
24  
25  
26  
27

28 For the analysed samples it is observed a non-uniform behaviour (Fig. 5 and 6).  
29 Observing the displacement field determined by digital image correlation, the values on  
30 central region of the samples are greater than those occurring on the side edges (Fig. 5).  
31 The displacement values are low, as expected due to low intensity loads applied in the  
32 samples. In this case, for the analyzed region the maximum value is 1.35 mm for sample  
33 1 (Fig. 5 (a)) where the applied displacement load was higher, 2.48 mm. Beholding the  
34 Fig. 5, it is possible to verify that the four samples have different displacement field  
35 distributions. Despite of that, samples 1 and 3 have a similar qualitative distribution of  
36 displacement field while samples 2 and 4 have a very different behavior for this  
37 parameter.  
38  
39  
40  
41  
42  
43  
44  
45  
46  
47  
48  
49  
50  
51  
52  
53  
54  
55  
56  
57  
58  
59  
60

(a)

(b)

(c)

(d)

1  
2  
3 Figure 5. Displacement field in y direction experimentally determined by DIC on:  
4 sample 1 (a), sample 2 (b), sample 3 (c), sample 4 (d).  
5  
6

7 The proposed numerical hybrid simulation used the displacement field obtained  
8 experimentally with DIC. Fig. 6 shows the displacement fields for the four models  
9 representing the simulation of the experimental tests previously performed. As  
10 expected, for most of the models, the displacement field of the hybrid method is very  
11 similar to the experimental using DIC. However, the displacement field of fourth  
12 sample has a different behavior from the experimental one which supplied the  
13 displacement field.  
14  
15  
16  
17  
18  
19  
20  
21  
22  
23  
24  
25  
26

27 (a) (b)  
28  
29  
30 (c) (d)  
31

32 Figure 6: Displacement field in y direction determined by the proposed hybrid method  
33 on: model 1 (a), model 2 (b), model 3 (c), model 4 (d).  
34  
35

36 One of the most important parameters to describe the mechanical behavior of  
37 materials is the strain. For this reason, the authors compared the variation of strains  
38 along a central line (dashed line in Fig. 5) for the three analyzed methods: DIC, FEM  
39 and hybrid. In Fig. 7 these strain variations are represented for the experimental  
40 samples and their respective simulated models using conventional FEM and the developed  
41 hybrid method. In both cases the Ogden constitutive model was used. Analyzing Fig. 7  
42 is possible to verify that the strains variation of experimental and hybrid methods are  
43 closer than those determined by FEM. Despite these similarities between the DIC  
44 results and hybrid simulation, between the sample and model 2 have noticed a  
45 significant deviation.  
46  
47  
48  
49  
50  
51  
52  
53  
54  
55  
56  
57  
58  
59  
60





Figure 7. Comparison among the three studied methods, DIC, FEM and hybrid, of strain variation along the vertical direction on the samples centres for: sample and model 1 (a), sample and model 2 (b), sample and model 3 (c), sample and model 4 (d).

#### 4. Discussion and conclusions

Figures 4 and 5 show the displacement field obtained with the experimental method (DIC) and determined by the hybrid method developed in this work. They demonstrate a similar global behaviour, despite some local variations which may be explained by the non uniform behaviour of human vaginal tissue.

In Fig. 7 it is observed, for the analysed samples, that the strain variation obtained with the hybrid method is closer to the experimental results than the traditional FEM simulation. The displacement variation of experimental and hybrid methods have the same trend, although in some samples important deviation occur, especially in regions further from the centre of the sample. In table 3 are indicated the average relative to DIC error for the FEM and hybrid method. During this work were done other relative error analyses for different values of displacements and the verified range of values were similar to the represented in Table 3, even in small displacements.

Table 3 – Average relative error.

Observing the table 3 it is possible to conclude that sample 1 and 3 have the lower average relative error and the classical FEM has high relative error when compared with the hybrid. So, the hybrid method developed in this work demonstrated

1  
2  
3 that it can be a valid alternative for the study of biological hyper-elastic tissues to the  
4  
5 traditional finite element method (FEM). This method describes with a good accuracy  
6  
7 the mechanical behavior of these materials. In future works will be possible to use the  
8  
9 described method to allow the development of more accuracy algorithms in FEM  
10  
11 software.  
12

### 13 14 15 16 17 18 19 20 21 22 23 24 25 26 27 28 29 30 31 32 33 34 35 36 37 38 39 40 41 42 43 44 45 46 47 48 49 50 51 52 53 54 55 56 57 58 59 60

**References**

- [1] MJ Muñoz, JA Bea, et al. 2008. An experimental study of the mouse skin behaviour: Damage and inelastic aspects. *Journal of Biomechanics*, 41(1): 93-99.
- [2] LL Gras, D Mitton, P Viot, S Laporte. 2010. Modelling of human muscle behaviour with a hyper-elastic constitutive law. *Computer Methods in Biomechanics and Biomedical Engineering*. 13(S1): 63-64.
- [3] JAC Martins, MP Pato, EB Pires, RM Jorge, M Parente, T Mascarenhas. 2007. Finite element studies of the deformation of the pelvic floor. *Ann NY Acad Sci*. 1101: 316–334.
- [4] CS Saleme, MPL Parente, et al. 2011. An approach on determining the displacements of the pelvic floor during voluntary contraction using numerical simulation and MRI. *Computer Methods in Biomechanics and Biomedical Engineering*. 14(4): 365-370.
- [5] GA Holzapfel, HW Weizsäcker. 1998. Biomechanical behavior of the arterial wall and its numerical characterization. *Computers in Biology and Medicine*. 28: 377-392.
- [6] J Afonso, P Martins, et al. 2008. Mechanical properties of polypropylene mesh used in pelvic floor repair. *International Urogynecol Journal*, 19: 375–380.
- [7] P Martins, R Jorge, A Ferreira. 2006. A Comparative Study of Several Material Models for Prediction of Hyperelastic Properties: Application to Silicone-Rubber and Soft Tissues. *Strain*. 42: 135–147.
- [8] M Sasso, G Palmieri, G Chiappini, D Amodio. 2008. Characterization of hyperelastic rubber-like materials by biaxial and uniaxial stretching tests based on optical methods. *Polymer Testing*. 27: 995–1004.
- [9] P Martins, E Peña, et al. 2010. Prediction of nonlinear elastic behaviour of vaginal tissue: experimental results and model formulation. *Computer Methods in Biomechanics and Biomedical Engineering*. 13 (3): 327–337.
- [10] B Calvo, E Peña, M A Martinez, M Doblaré. 2007. An uncoupled directional damage model for fibred biological soft tissues. Formulation and computational aspects. *International Journal for Numerical Methods in Engineering*. 69(10):2036–2057.
- [11] L Taber. 2004. *Nonlinear Theory of Elasticity: Applications in Biomechanics*. World Scientific Publishing, London.
- [12] H G. A. Holzapfel. 2000. *Nonlinear Solid Mechanics: Continuum Approach for Engineering*, John Wiley & Sons Ltd, West Sussex, England.
- [13] AE Green and JE. Adkins. 1970. *Large Elastic Deformations*. 2nd Ed., Oxford University Press, London.
- [14] M. Sutton, J. Wolters, H. Peters, F. Ranson and R. McNeil. 1983. Determination of

- 1  
2  
3 Displacements Using an Improved Digital Correlation Method. *Image and Vision*  
4 *Computing*. 1: 133-139.
- 5 [15] M. Sutton, Q. Cheng, H. Peters, J. Chao and R. McNeill. 1986. Application of an  
6 Optimized Digital Correlation Method to Planar Deformation Analysis. *Image and*  
7 *Vision Computing*. 4: 143-151.
- 8 [16] M. Sutton, L. Turner, A. Bruck, and A. Chae. 1991. Full-field Representation of  
9 Discretely Sampled Surface Deformation for Displacement and Strain Analysis,  
10 *Experimental Mechanics*. 31: 168-177.
- 11 [17] M. Sutton, R. McNeill, J. Jang, and M. Babai. 1988. Effects of Subpixel Image  
12 Restoration on Digital Correlation Error. *Journal of Optical Engineering*. 27: 870-  
13 877.
- 14 [18] A. Bruck, R. McNeil, M. Sutton, and H. Peters. 1989. Digital Image Correlation  
15 Using Newton-Raphson Method of Partial Differential Correction. *Experimental*  
16 *Mechanics*. 29: 261-267.
- 17 [19] T. Hu, W. Ranson, M. Sutton and W. Peters. 1985. Application of Digital Image  
18 Correlation Techniques to Experimental Mechanics, *Experimental Mechanics*, 25:  
19 232-244.
- 20 [20] D. Lecompte, et Al. 2006. Quality assessment of speckle patterns for digital image  
21 correlation, *Optics and Lasers in Engineering*, 44: 1132–1145.
- 22 [21] P. Hung and A. Voloshin. 2003. In-plane Strain Measurement by Digital Image  
23 Correlation. *Journal of the Brazilian Society of Mechanical Sciences and*  
24 *Engineering*. 25: 215-221.
- 25 [22] H. Marcellierl, P. Vescovo, et al. 2001. Optical analysis of displacement and strain  
26 fields on human skin. *Skin Research and Technology*. 7: 246-253.
- 27 [23] M. Mooney. 1940. A theory of large elastic deformation. *Journal of Applied*  
28 *Physics*. 11(9): 582-592.
- 29 [24] R. W. Ogden. 1972. Large Deformation Isotropic Elasticity - On the Correlation of  
30 Theory and Experiment for Incompressible Rubberlike Solids. *Proceedings of the*  
31 *Royal Society of London. Series A, Mathematical and Physical Sciences*,  
32 326(1567): 565-584.
- 33 [25] O. H. Yeoh. 1993. Some forms of the strain energy function for rubber. *Rubber*  
34 *Chemistry and technology*, 66(5): 754-771.
- 35 [26] R. Ogden. 1984. *Non-Linear Elastic Deformations*. Dover Publications.
- 36 [27] O. Zienkiewicz, R. Taylor. 1991. *The finite element method*, McGraw Hill, Oxford.
- 37 [28] ANSYS – Theory Reference, Edited by Peter Kohnke, 1999.
- 38  
39  
40  
41  
42  
43  
44  
45  
46  
47  
48  
49  
50  
51  
52  
53  
54  
55  
56  
57  
58  
59  
60